Supporting Information

for

Corannulene derivatives with low LUMO levels and dense convex–concave packing for n-channel organic field-effect transistors

Rui Chen,[a] Ru-Qiang Lu,[a] Ke Shi,[b] Fan Wu,[a] Hong-Xun Fang,[a] Zhe-Xuan Niu,[a] Xiao-Yun Yan,[a] Ming Luo,[a] Xin-Chang Wang,[a] Chi-Yuan Yang,[b] Xiao-Ye Wang,[b] Binbin Xu,[c] Haiping Xia,[a] Jian Pei[b] and Xiao-Yu Cao[a]*

[a] State Key Laboratory of Physical Chemistry for Solid Surfaces, College of Chemistry and Chemical Engineering, Xiamen University, Xiamen 361005 (P. R. China), E-mail: xcao@xmu.edu.cn.

[b] Beijing National Laboratory for Molecular Sciences (BNLMS), the Key Laboratory of Bioorganic Chemistry and Molecular Engineering of Ministry of Education, College of Chemistry and Molecular Engineering, Peking University, Beijing 100871 (P. R. China).

[c] Center of Instrumental Analysis, College of Chemistry and Chemical Engineering, Xiamen University, Xiamen, China.

Table of Contents

1. Instruments and Materials

General. All commercially available chemicals were used without further purification unless otherwise noted. 1-Methyl-2-pyrrolidinone (NMP) was dried for 24 hours with P_2O_5 and distilled under reduced pressure and prior to use. ^{1}H and ^{13}C NMR spectra were recorded on Bruker AVIII-500. Chemical shifts were reported in ppm. Coupling constants (*J* values) were reported in Hertz. ^{1}H NMR chemical shifts were referenced to $CDCl_3$ (7.26 ppm). ^{13}C NMR chemical shifts were referenced to $CDCl_3$ (77.0 ppm). High-resolution mass spectra (HRMS) were recorded on a Bruker En Apex Ultra 7.0T FT-MS mass spectrometer. Elemental analyses were performed using

a German Vario EL III elemental analyzer. Thermal gravity analyses (TGA) were carried out on a NETZSCH TG 209F1 Iris analyzer at a rate of 10 °C min^{-1} from room temperature to 800 °C under nitrogen atmosphere.

Absorption spectra were recorded on Shimadzu UV2550 UV-*vis* spectrometer. Cyclic voltammetry (CV) was performed on BASI Epsilon workstation and measurements were carried out in dichloromethane containing n-Bu_4NPF_6 (0.1 M) as supporting electrolyte. A platinum wire was used as a counter electrode and glassy carbon electrode as a working electrode, all potentials were recorded versus Ag/AgCl (saturated) as a reference electrode. The scan rate was 100 $mV.s^{-1}$. Transmission electron microscopy (TEM) studies were performed on a JEM-2100 high-resolution transmission electron microscope operating at 200 kV. Samples were prepared by dropping dispersion of samples onto carbon-coated copper grids and immediately evaporating the solvent. The morphology was characterized by Hitachi-S4800 scanning electron microscopy.

2. Synthetic Procedures.

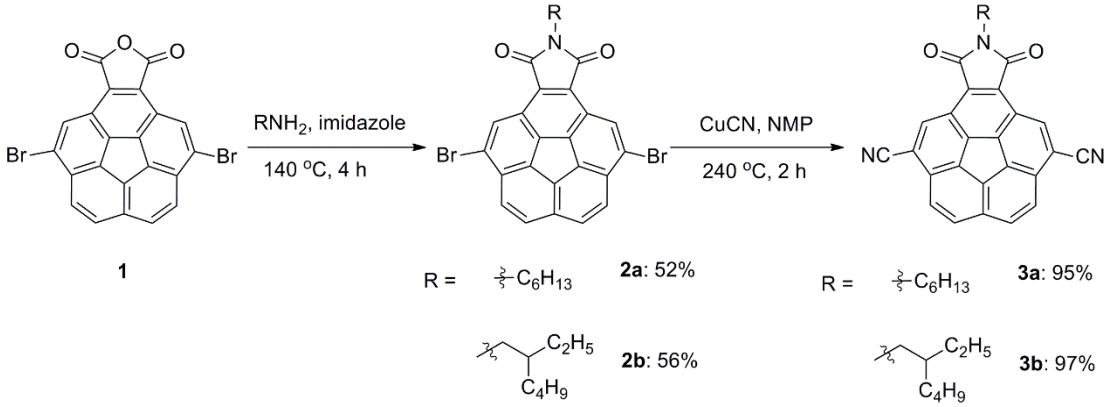

Compound 2a. Compound **2a** was synthesized according to literature methods.[1,2] Compound **1** (1.00 g, 2.10 mmol), imidazole (1.43 g, 21.0 mmol), and *n*-hexylamine (0.234 g, 2.31 mmol) were mixed and heated to 140 °C for 4 hours under nitrogen. The reaction mixture was then allowed to cool to room temperature and 5% HCl (60 mL) and ethanol (30 mL) were added. The mixture was stirred at room temperature for 2 hours. The mixture was next extracted with dichloromethane, washed with water, dried with Na_2SO_4 and filtered. The filtrate was evaporated and the crude product was purified by column chromatography over silica gel (PE:DCM=4:1) and recrystallization from CH_3OH/CH_2Cl_2 to provide the title product (611 mg, yield 52%). ^1H NMR (500 MHz, $CDCl_3$, 298 K, ppm): δ 8.59 (s, 2H), 7.95 – 7.89 (AB, $\Delta\nu$ = 21.5 Hz, J = 9.00 Hz, 4H), 3.74 (t, J = 7.0 Hz, 2H), 1.75 – 1.68 (m, 2H), 1.39 – 1.28 (m, 6H), 0.88 (t, J = 6.0 Hz, 3H); ^{13}C NMR (126 MHz, $CDCl_3$, 298 K, ppm): δ 168.25, 136.05, 133.56, 132.92, 130.68, 130.57, 130.37, 129.23, 127.61, 127.29, 124.75, 124.15, 38.03, 31.38, 28.76, 26.57, 22.54, 14.05.; ESI-HRMS *m/z*: Calcd. for $[C_{28}H_{19}Br_2NO_2+H]^+$: 561.9837; Found: 561.9832.

Compoud 2b. Compound **1** (1.00 g, 2.10 mmol), imidazole (1.43 g, 21.0 mmol), and 2-ethylhexylamine (0.299 g, 2.31 mmol） were mixed and heated to 140 °C for 4 hours under nitrogen. The reaction mixture was then allowed to cool to room temperature and 5% HCl (60 mL) and ethanol (30 mL) were added. The mixture was stirred at room temperature for 2 hours. The mixture was next extracted with dichloromethane, washed with water, dried with Na_2SO_4 and filtered. The filtrate was evaporated and the crude product was purified by column chromatography over silica gel (PE:DCM=4:1) and recrystallization from CH_3OH/CH_2Cl_2 to

provide the title product (691 mg, yield 56%). ^{1}H NMR (500 MHz, $CDCl_3$, 298 K, ppm): δ 8.60 (s, 2H), 7.95 –7.91 (AB, Δ*v* = 21 Hz, *J* = 8.75 Hz, 4H), 3.64 (d, *J* = 7.2 Hz, 2H), 1.90 – 1.82 (m, 1H), 1.42 – 1.27 (m, 8H), 0.94 (t, *J* = 7.4 Hz, 3H), 0.90 (t, *J* = 6.7 Hz, 3H).; ^{13}C NMR (126 MHz, $CDCl_3$, 298 K, ppm): δ 168.62, 136.29, 133.75, 133.10, 130.80, 130.69, 130.43, 129.30, 127.73, 127.34, 124.93, 124.20, 41.78, 38.70, 30.65, 28.64, 23.96, 23.02, 14.11, 10.50.; ESI-HRMS *m/z*: Calcd. for $[C_{30}H_{23}O_2Br_2N+H]^+$: 590.0150; Found: 590.0143.

Compoud 3a. Compound **3a** was synthesized according to literature methods with slight modifications[3] . A mixture of **2a** (100 mg, 0.179 mmol) and CuCN (223 mg, 2.50 mmol) in anhydrous NMP (10.0 mL) was heated to 240 °C for 2 hours under nitrogen. After the solvent was removed under reduced pressure, CH_2Cl_2 (10 mL) was added to dissolve the residue. The mixture was filtered and the solvent was evaporated. The crude product was purified by column chromatography over silica gel (PE:DCM=1:1) and recrystallization from CH_3OH/CH_2Cl_2 to provide the title product (77.1 mg, yield 95%) as a yellow solid. ^{1}H NMR (500 MHz, $CDCl_3$, 298 K, ppm): δ 8.91 (s, 2H), 8.05 – 8.11 (AB, Δ*v* = 30.5 Hz, *J* = 8.75 Hz, 4H), 3.78 (t, *J* = 7.3 Hz, 2H), 1.76 – 1.67 (m, 2H), 1.39-1.31 (m, 6H), 0.88 (t, *J* = 6.5 Hz, 3H).; ^{13}C NMR (126 MHz, $CDCl_3$, 298 K, ppm): δ 167.78, 138.80, 135.13, 134.43, 133.63, 132.21, 132.10, 130.84, 130.32, 126.36, 124.12, 116.18, 113.27, 38.38, 31.29, 28.63, 26.48, 22.47, 13.99.; UV-vis (DCM) λ nm (ε, M^{-1} cm^{-1}) 317 (54200), 256 (49600). ESI-HRMS *m/z*: Calcd. for $[C_{30}H_{19}N_3O_2+H]^+$: 454.1550; Found: 454.1548. Elemental Anal. Calcd. for $C_{30}H_{19}N_3O_2$: C, 79.46; H, 4.22; N, 9.27; Found: C, 79.63; H, 4.25; N, 9.30.

Compoud 3b. A mixture of **2b** (200 mg, 0.341 mmol) and CuCN (424 mg, 4.77 mmol) in anhydrous NMP (20.0 mL) was heated to 240 °C for 2 hours under nitrogen. After the solvent was removed under reduced pressure, CH_2Cl_2 (20 mL) was added to dissolve the residue. The mixture was filtered and the solvent was evaporated. The crude product was purified by column chromatography over silica gel (PE:DCM=1:1) and recrystallization from CH_3OH/CH_2Cl_2 to provide the title product (159 mg, yield 97%) as a yellow solid. ^{1}H NMR (500 MHz, $CDCl_3$, 298 K, ppm): *δ* 8.89 (s, 2H), 8.10 – 8.04 (AB, Δ*v* = 29 Hz, *J* = 9.00 Hz, 4H), 3.68 (d, *J* = 7.0 Hz,2H), 1.89 – 1.84 (m, *J* = 24.5 Hz, 1H), 1.39-1.31 (m, 8H), 0.94 (t, *J* = 7.4 Hz, 3H), 0.90 (t, *J* = 6.8 Hz, 3H); ^{13}C NMR (126 MHz, $CDCl_3$, 298 K, ppm): δ 168.19, 139.15, 135.43, 134.76, 133.79, 132.38, 132.14, 130.88, 130.53, 126.44, 124.32, 116.29, 113.38, 42.15, 38.59, 30.55, 28.53, 23.88, 22.96, 14.06, 10.43.; UV-vis (DCM) λ nm (ε, M^{-1} cm^{-1}) 318 (54900), 256 (49800). ESI-HRMS *m/z*: Calcd. for $[C_{32}H_{23}O_2N_3$ $+H]^+$: 482.1863; Found: 482.1864. Elemental Anal. Calcd. for $C_{32}H_{23}N_3O_2$: C, 79.81; H, 4.81; N, 8.73; Found: C, 80.06; H, 4.80; N, 8.75.

3. Thermogravimetric Analysis (TGA)

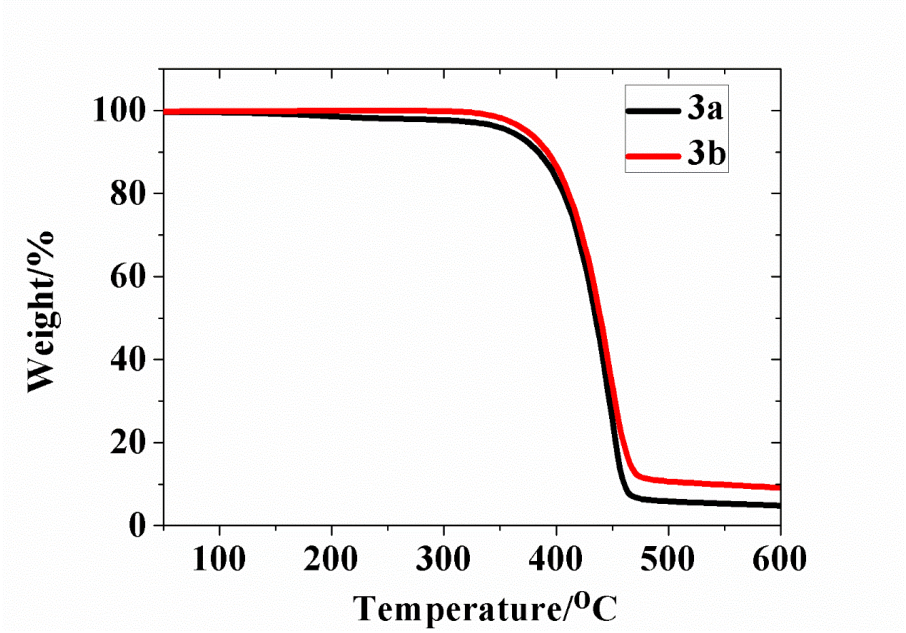

Figure S1. TGA plot of **3a** (5% loss, 350 °C) and **3b** (5% loss, 373 °C).

4. Concentration-Dependent ^{1}H NMR Spectra

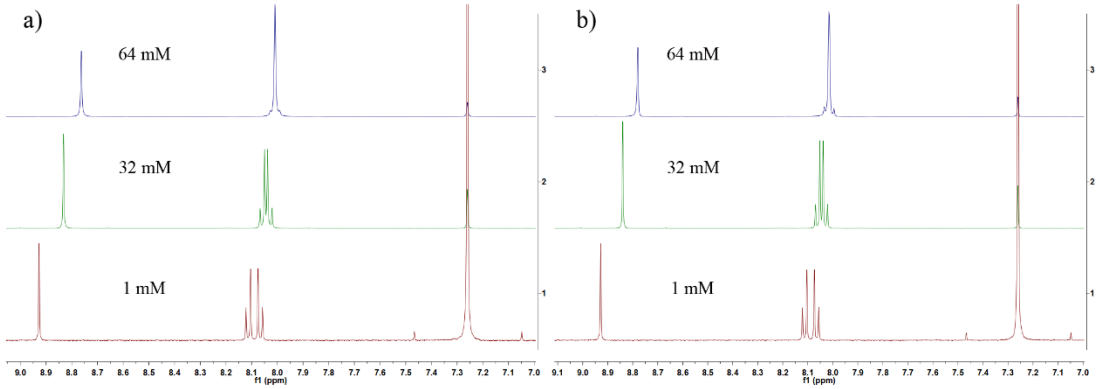

Figure S2. Concentration-dependent ^{1}H NMR spectra of **3a** a) and **3b** b) (500 MHz, $CDCl_3$, 298 K, ppm).

5. SEM images

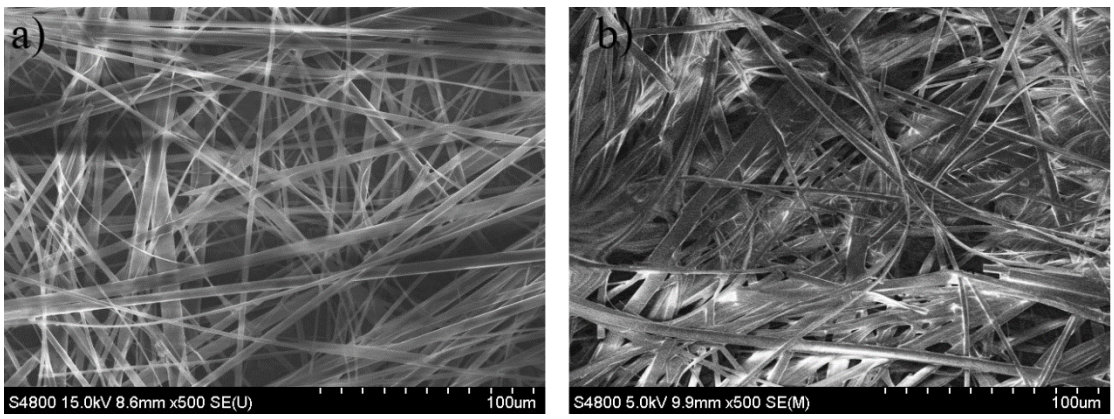

Figure S3. SEM images of **3a** a) and **3b** b).

6. X-ray powder diffraction

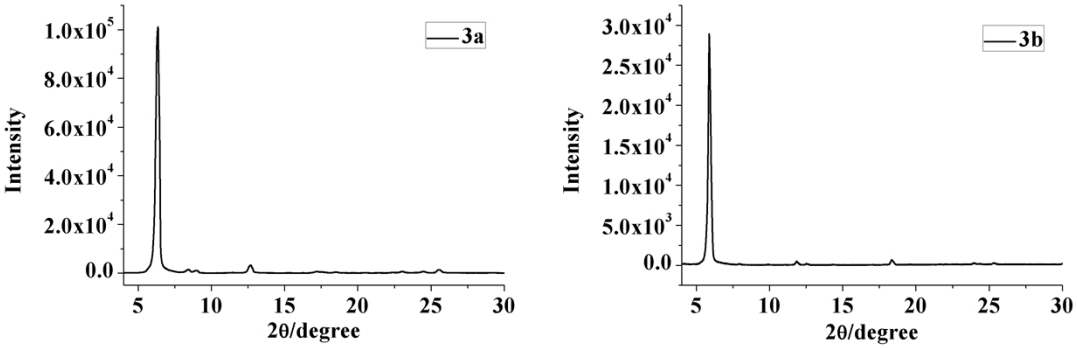

Figure S4. X-ray powder diffraction data of **3a** and **3b**.

7. Computational Studies

The geometries of cyanated imide-fused corannulene were optimized at the B3LYP/6-31G(d) level, and the HOMO and LUMO were then calculated with the 6-311+G(d,p) basis set, using the Ganssian 09 software package.[4] The intermolecular couplings were evaluated by the general gradient functional GGA in conjunction with the PBE gradient corrections with the double-ζ plus polarization (DZP) basis set using the Amsterdam Density Functional (ADF) program package.[5,6,7] The methodology used for charge transfer properties is direct method by using ADF's unique fragment approach. ADF allows one to use molecular orbitals on individual molecules as a basis set in calculations on a system composed of two or more molecules. The charge transfer integrals obtained in this way differ significantly from values estimated from the energy splitting between the highest occupied molecular orbitals in a dimer. The difference is due to the nonzero spatial overlap between the molecular orbitals on adjacent molecules. Additionally, ADF's methods are applicable to cases where an orbital on one molecule couples with two or more orbitals on another molecule (From http://www.scm.com/ADF/).

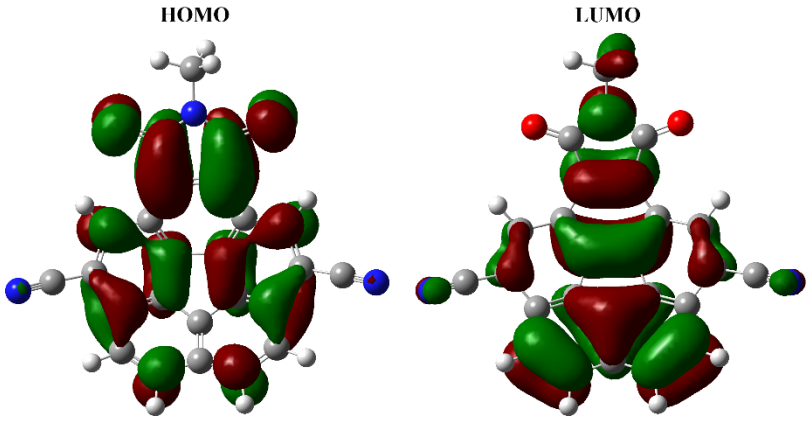

Figure S5. Calculated HOMO and LUMO of cyanated imide-fused corannulene.

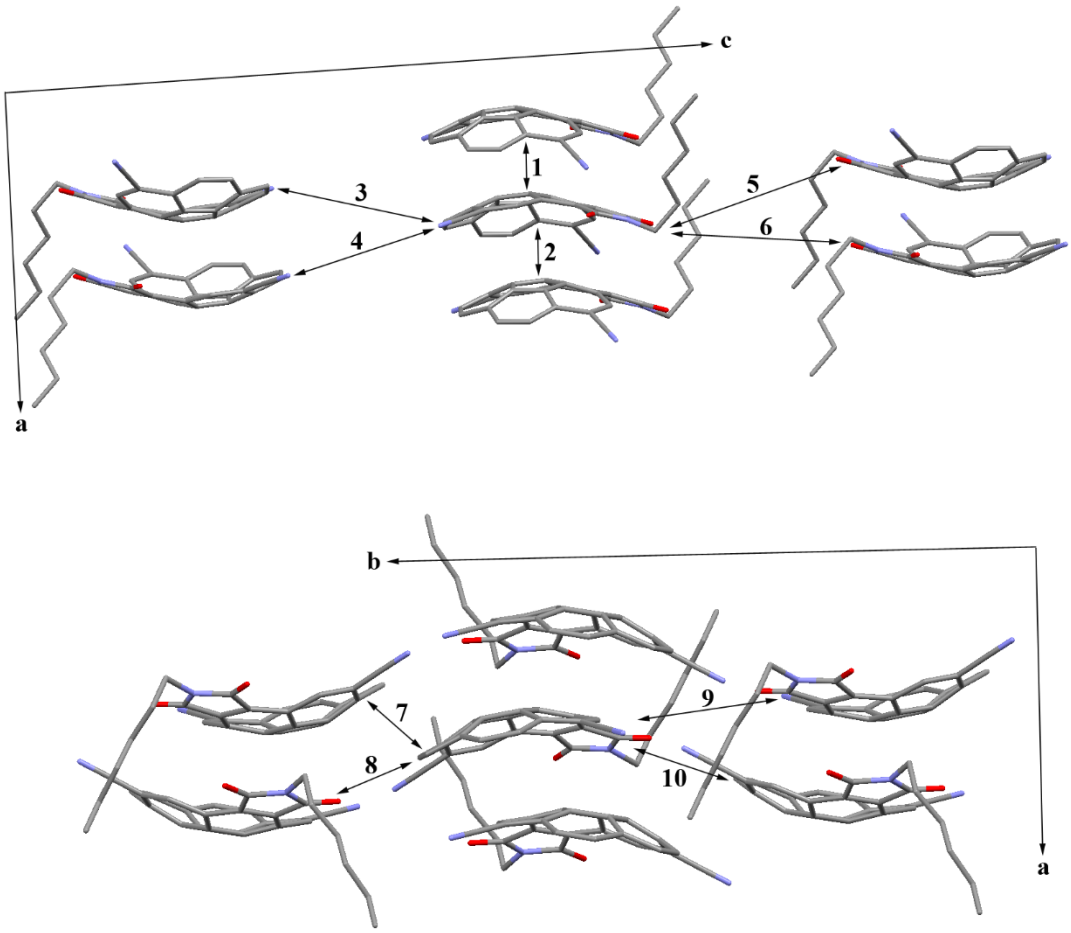

Figure S6. Electronic couplings V (meV) in the single crystal of **3a.**

Table S1. Calculation of electronic couplings V (meV) for hole transfer integrals and electron transfer integrals in the single crystal of **3a**

Route	J_{RP}(eV)[a]	S_{RP}[b]	H_{RR}(eV)[c]	H_{pp}(eV)[c]	$V_{HOMO/LUMO}$(eV)[d]	$V_{HOMO/LUMO}$(meV)
1 $_{hole}$	0.02962	-0.00290	-7.44395	-7.50716	0.007940957	7.940957283
1 $_{electron}$	0.05977	-0.00696	-4.94858	-5.06449	0.024925724	24.925723842
2 $_{hole}$	-0.02515	0.00219	-7.24194	-7.30556	-0.009220532	-9.220531723
2 $_{electron}$	0.04955	-0.00578	-4.91071	-4.87833	0.021260385	21.260384675
3 $_{hole}$	0.00009	-0.00001	-7.34698	-7.40618	0.000016234	0.016234200
3 $_{electron}$	0.00000	0.00000	-4.90537	-4.90528	0.000000000	0.000000000
4 $_{hole}$	-0.00016	0.00002	-7.42188	-7.42200	-0.000011561	-0.011561200
4 $_{electron}$	0.00002	0.00000	-4.92362	-4.92346	0.000020000	0.020000000
5 $_{hole}$	0.00008	-0.00001	-7.39856	-7.39866	0.000006014	0.006013900
5 $_{electron}$	-0.00004	0.00000	-4.89928	-4.89940	-0.000040000	0.040000000

6 $_{hole}$	-0.00018	0.00002	-7.14594	-7.43627	-0.000034178	-0.034177900
6 $_{electron}$	0.00001	0.00000	-4.72980	-4.92924	0.000010000	0.010000000
7 $_{hole}$	-0.00525	0.00047	-7.16217	-7.16211	-0.001883795	-1.883794616
7 $_{electron}$	-0.05243	0.00522	-4.73827	-4.73846	-0.027696489	-27.696489385
8 $_{hole}$	-0.00292	0.00023	-7.23211	-7.14501	-0.001266631	-1.266631267
8 $_{electron}$	-0.00032	-0.00006	-4.72387	-4.74722	-0.000604133	-0.604132702
9 $_{hole}$	0.00075	-0.00006	-7.11936	-7.11947	0.000322835	0.322835101
9 $_{electron}$	-0.00006	0.00000	-4.73771	-4.73756	-0.000060000	-0.060000000
10 $_{hole}$	-0.00294	0.00024	-7.14518	-7.23194	-0.001214746	-1.214745670
10$_{electron}$	-0.00031	-0.00006	-4.74705	-4.72403	-0.000594132	-0.594132402

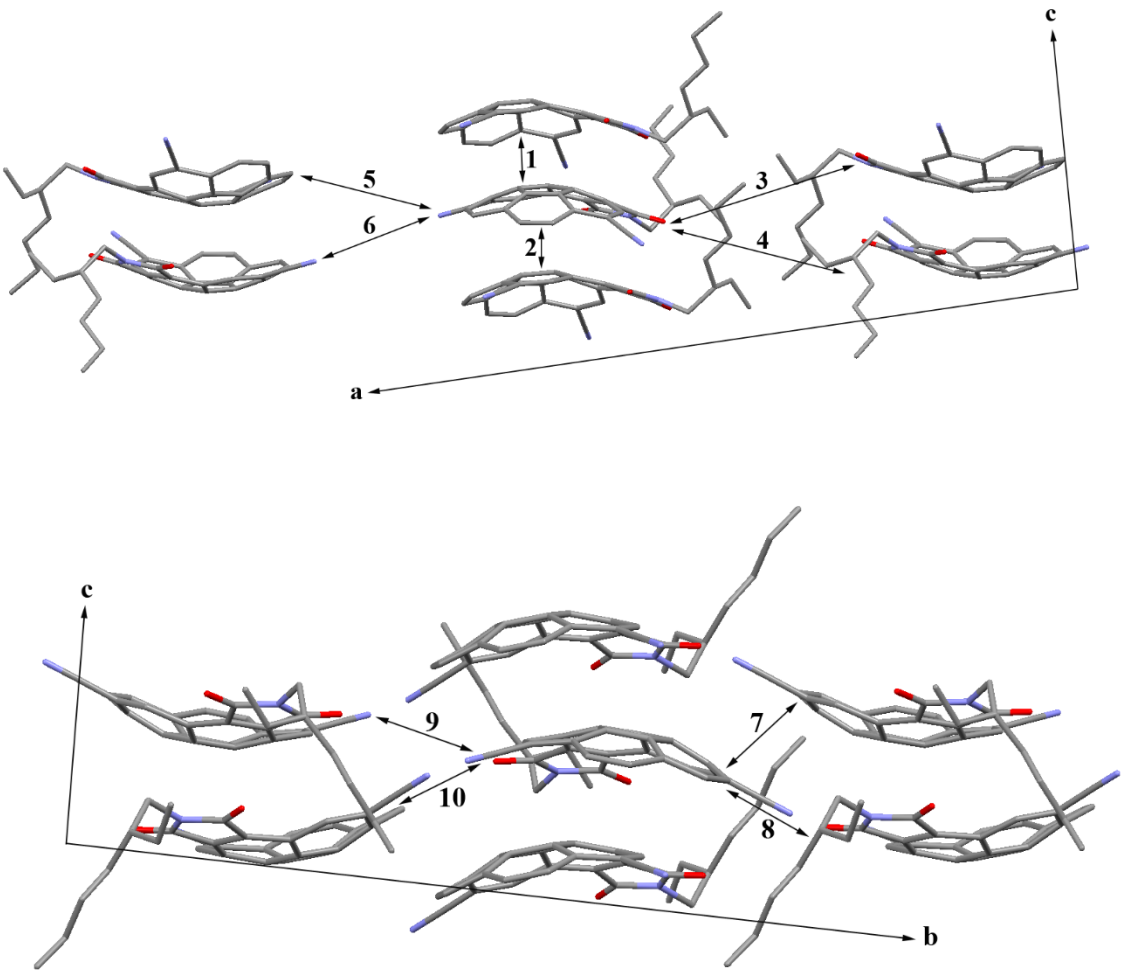

Figure S7. Electronic couplings V (meV) in the single crystal of **3b.**

Table S2. Calculation of electronic couplings V (meV) for hole transfer integrals and electron transfer integrals in the single crystal of **3b**

Route	J_{RP}(eV)[a]	S_{RP}[b]	H_{RR}(eV)[c]	H_{pp}(eV)[c]	$V_{HOMO/LUMO}$(eV)[d]	$V_{HOMO/LUMO}$(meV)
1 $_{hole}$	0.02611	-0.00231	-7.31688	-7.27680	0.009254349	9.254348982
1 $_{electron}$	-0.03310	0.00436	-4.87647	-4.91333	-0.011758460	-11.758459524
2 $_{hole}$	0.02617	-0.00232	-7.31697	-7.27680	0.009241277	9.241276540
2 $_{electron}$	-0.03310	0.00436	-4.87650	-4.91330	-0.011758460	-11.758459524
3 $_{hole}$	-0.00096	0.00007	-7.21704	-7.21713	-0.000454804	-0.454804052
3 $_{electron}$	0.00007	-0.00001	-4.77445	-4.77438	0.000022256	0.022255850
4 $_{hole}$	0.00010	0.00000	-7.19073	-7.19073	0.000100000	0.100000000
4 $_{electron}$	-0.00001	0.00000	-4.76080	-4.76080	0.000010000	0.010000000
5 $_{hole}$	0.00005	-0.00001	-7.17906	-7.17915	0.000021791	0.021791050
5 $_{electron}$	0.00005	-0.00001	-4.75809	-4.75810	0.000002419	0.002419050
6 $_{hole}$	0.00001	0.00000	-7.17962	-7.17961	0.000010000	0.010000000
6 $_{electron}$	-0.00001	0.00000	-4.75206	-4.75213	0.000010000	0.010000000
7 $_{hole}$	0.00152	-0.00016	-7.17491	-7.17485	0.000372019	0.372019210
7 $_{electron}$	-0.05844	0.00583	-4.73722	-4.73723	-0.030823026	-30.823025891
8 $_{hole}$	-0.00672	0.00056	-7.16834	-7.23593	-0.002686805	-2.686805243
8 $_{electron}$	0.00144	-0.00022	-4.74949	-4.72125	0.000398219	0.398218619
9 $_{hole}$	-0.00017	0.00001	-7.14376	-7.14367	-0.000098563	-0.098562850
9 $_{electron}$	0.00004	0.00000	-4.73925	-4.73927	0.000040000	0.040000000
10 $_{hole}$	-0.00688	0.00057	-7.23591	-7.16843	-0.002774764	-2.774764002
10$_{electron}$	0.00144	-0.00022	-4.72127	-4.74947	0.000398219	0.398218619

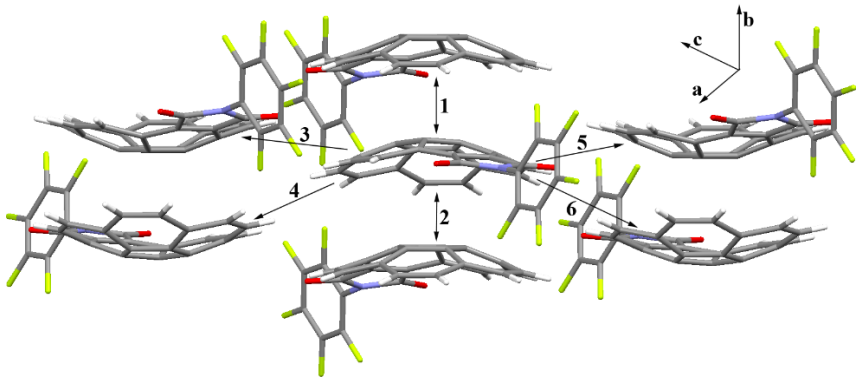

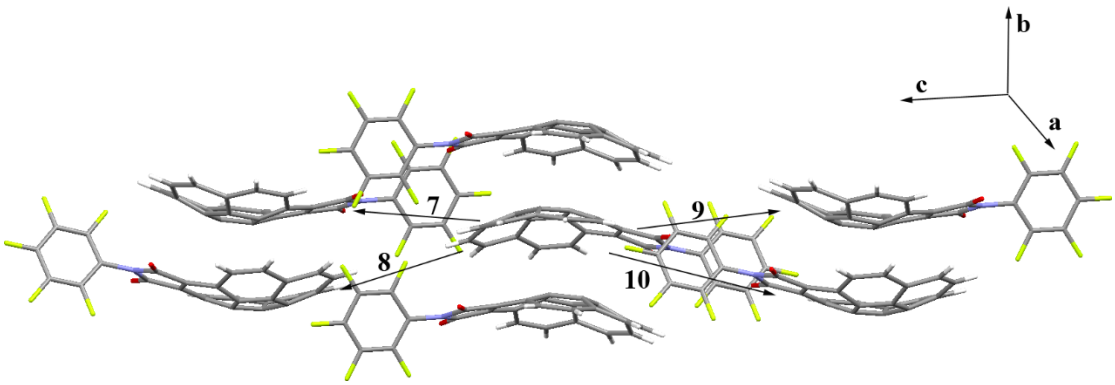

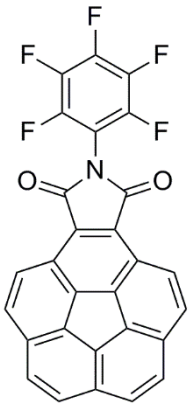

Imide-fused corannlene

Figure S8. Electronic couplings V (meV) in the single crystal of imide-fused corannulene.[8]

Table S3. Calculation of electronic couplings V (meV) for hole transfer integrals and electron transfer integrals in the single crystal of imide-fused corannulene.

Route	J_{RP}(eV)[a]	S_{RP}[b]	H_{RR}(eV)[c]	H_{pp}(eV)[c]	$V_{HOMO/LUMO}$(eV)[d]	$V_{HOMO/LUMO}$(meV)
1 $_{hole}$	0.01835	-0.00290	-6.93035	-6.83759	-0.001613527	-1.613526570
1 $_{electron}$	-0.19097	0.02032	-4.58758	-4.46492	-0.099037493	-99.037492818
2 $_{hole}$	0.01848	-0.00291	-6.93029	-6.83753	-0.001552191	-1.552191244
2 $_{electron}$	-0.19098	0.02033	-4.58764	-4.46480	-0.099002866	-99.002866166
3 $_{hole}$	0.02220	-0.00199	-6.80449	-6.96985	0.008494565	8.494565339
3 $_{electron}$	-0.00419	0.00044	-4.42207	-4.58115	-0.002209292	-2.209292028
4 $_{hole}$	-0.00329	0.00037	-6.95367	-6.95382	-0.000717114	-0.717114448
4 $_{electron}$	-0.00023	0.00003	-4.56463	-4.56475	-0.000093059	-0.093059300
5 $_{hole}$	-0.02221	0.00199	-6.80446	-6.96989	-0.008504555	-8.504555429
5 $_{electron}$	-0.00419	0.00044	-4.42196	-4.58125	-0.002209294	-2.209294228
6 $_{hole}$	-0.01290	0.00137	-6.83926	-6.83925	-0.003530227	-3.530227276
6 $_{electron}$	-0.00088	0.00012	-4.52815	-4.52830	-0.000336613	-0.336613005

7 $_{\text{hole}}$	-0.00019	0.00003	-6.77101	-6.91803	0.000015336	0.015335600
7 $_{\text{electron}}$	0.00175	-0.00016	-4.39591	-4.56403	0.001033205	1.033204826
8 $_{\text{hole}}$	0.00057	-0.00006	-6.93036	-6.93035	0.000154179	0.154178701
8 $_{\text{electron}}$	-0.00023	0.00003	-4.53600	-4.53616	-0.000093918	-0.093917600
9 $_{\text{hole}}$	0.00019	-0.00003	-6.77094	-6.91809	-0.000015335	-0.015335450
9 $_{\text{electron}}$	0.00175	-0.00016	-4.39578	-4.56415	0.001033206	1.033205626
10 $_{\text{hole}}$	-0.00070	-0.00001	-6.78883	-6.78901	-0.000767889	-0.767889200
10$_{\text{electron}}$	-0.00074	0.00005	-4.43100	-4.43115	-0.000518446	-0.518446251

[a)] J_{RP}: charge transfer integral; [b)] S_{RP}: overlap integral; [c)] H_{RR} and H_{PP}: site integral; [d)] $V=[J_{RP}-0.5S_{RP}(H_{RR}+H_{PP})]/(1-S_{RP}^2)$, V_{HOMO} for hole transfer integrals and V_{LUMO} for electron transfer integrals.

8. Single Crystal Data

Single crystals suitable for X-ray analysis were obtained through vapor diffusion of methanol into THF solutions.

Table S4. Crystal data and structure refinement for **3a**

Empirical formula	$C_{30}H_{19}N_3O_2$
Formula weight	453.48
Temperature/K	173(2)
Crystal system	monoclinic
Space group	I2/a
a/Å	7.2119(4)
b/Å	21.7175(15)
c/Å	31.966(2)
α/°	90
β/°	95.488(6)
γ/°	90
Volume/Å^3	4983.7(5)
Z	8
ρ_{calc}g/cm^3	1.209
μ/mm^{-1}	0.616
F(000)	1888.0
Crystal size/mm^3	0.4 × 0.2 × 0.1
Radiation	CuKα (λ = 1.54184)
2Θ range for data collection/°	8.142 to 124.292
Index ranges	$-8 \le h \le 8$, $-22 \le k \le 24$, $-36 \le l \le 35$
Reflections collected	10586
Independent reflections	3918 [R_{int} = 0.1340, R_{sigma} = 0.0989]

Data/restraints/parameters	3918/0/317
Goodness-of-fit on F^2	1.014
Final R indexes [I>=2σ (I)]	R_1 = 0.0776, wR_2 = 0.1974
Final R indexes [all data]	R_1 = 0.0862, wR_2 = 0.2105
Largest diff. peak/hole / e Å^{-3}	0.36/-0.43

Table S5. Crystal data and structure refinement for **3b**

Empirical formula	$C_{34}H_{22.47}N_3O_{2.5}$
Formula weight	513.02
Temperature/K	173.0
Crystal system	monoclinic
Space group	C2/c
a/Å	33.040(3)
b/Å	21.8380(18)
c/Å	7.2037(7)
α/°	90
β/°	95.946(9)
γ/°	90
Volume/Å^3	5169.8(8)
Z	8
ρ_{calc}g/cm^3	1.318
μ/mm^{-1}	0.084
F(000)	2140.0
Crystal size/mm^3	0.2 × 0.1× 0.1
Radiation	MoKα (λ = 0.71073)
2Θ range for data collection/°	5.99 to 47.63
Index ranges	-43 ≤ h ≤ 40, -20 ≤ k ≤ 27, -9 ≤ l ≤ 9
Reflections collected	12299
Independent reflections	5844 [R_{int} = 0.0707, R_{sigma} = 0.1509]
Data/restraints/parameters	3970/8/365
Goodness-of-fit on F^2	1.051
Final R indexes [I>=2 σ (I)]	R_1 = 0.0762, wR_2 = 0.1596
Final R indexes [all data]	R_1 = 0.1189, wR_2 = 0.1813
Largest diff. peak/hole / e Å^{-3}	0.46/-0.26

9. Device Fabrication and Characterization

Bottom-gate/top-contact field-effect transistor devices were fabricated using n^{++}-Si/SiO_2 (300 nm) substrates. The substrates were cleaned by acetone, detergent, deionized water (twice) and iso-propanol for 10 min respectively and then dried in vacuum oven at 80 ^oC for 1 h. The substrates were modified with polystyrene solution (6 mg.mL^{-1} in toluene). The thickness of PS layer was measured to be 20 nm. The microwires suspensions of **3a** and **3b** in isopropanol were

spin-coated on substrates and annealed at 60 °C in vacuum overnight. The shadow mask were made as reported. Gold was deposited as drain and source electrodes with a thickness of 400 Å. All devices were measured by a Keithley 4200 parameter analyzer on a probe stage under ambient condition. The mobility was estimated in the saturated regime.

10. ^{1}H NMR and ^{13}C NMR Spectra

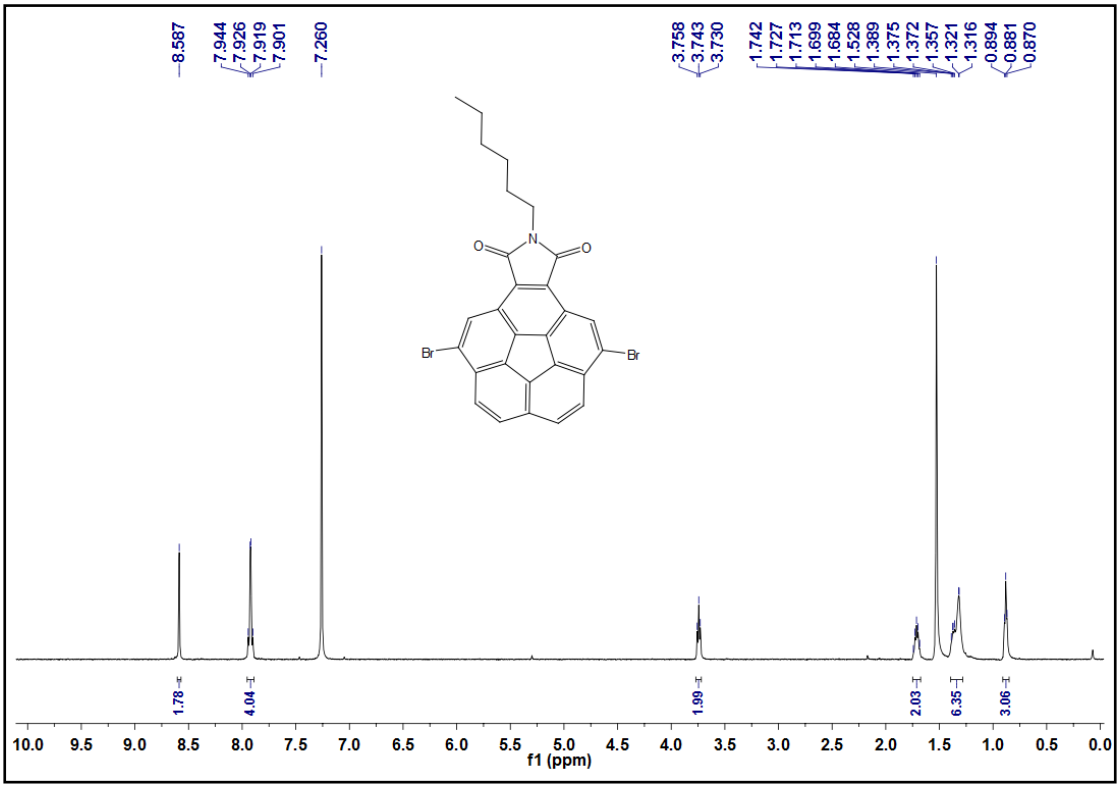

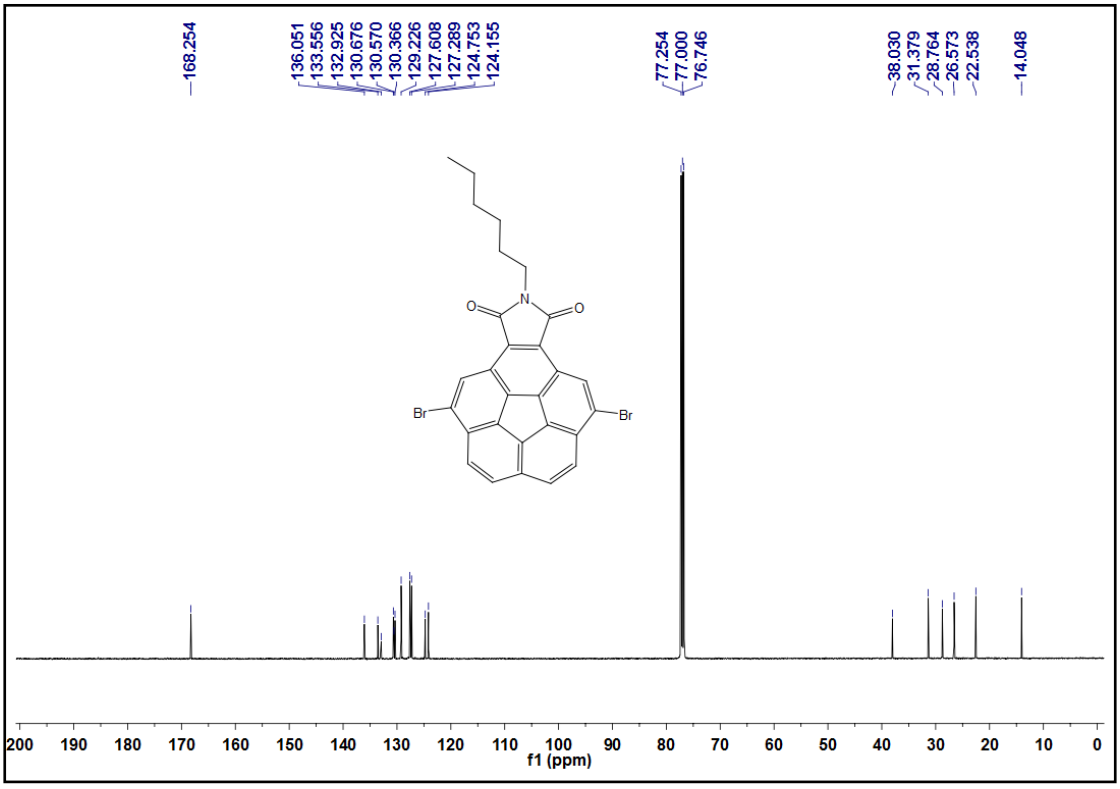

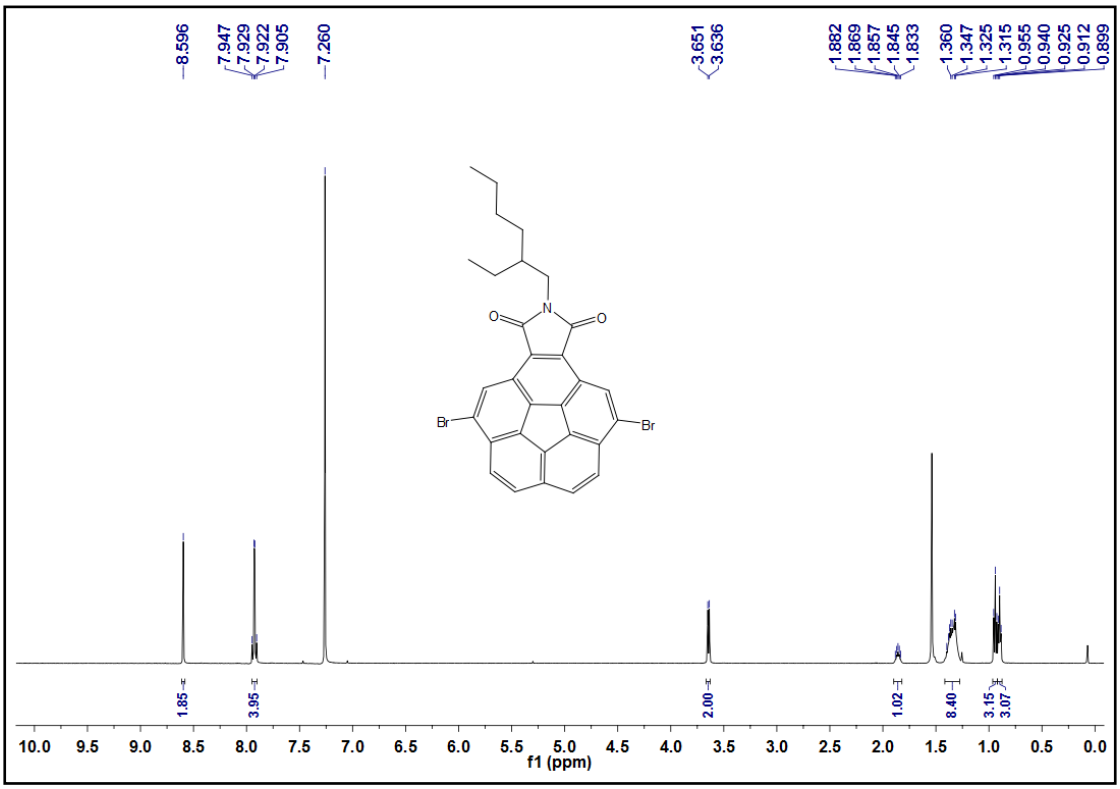
8.596
7.947
7.929
7.922
7.905
7.260
3.651
3.636
1.882
1.869
1.857
1.845
1.833
1.360
1.347
1.325
1.315
0.955
0.940
0.925
0.912
0.899
1.85
3.95
2.00
1.02
8.40
3.15
3.07
f1 (ppm)

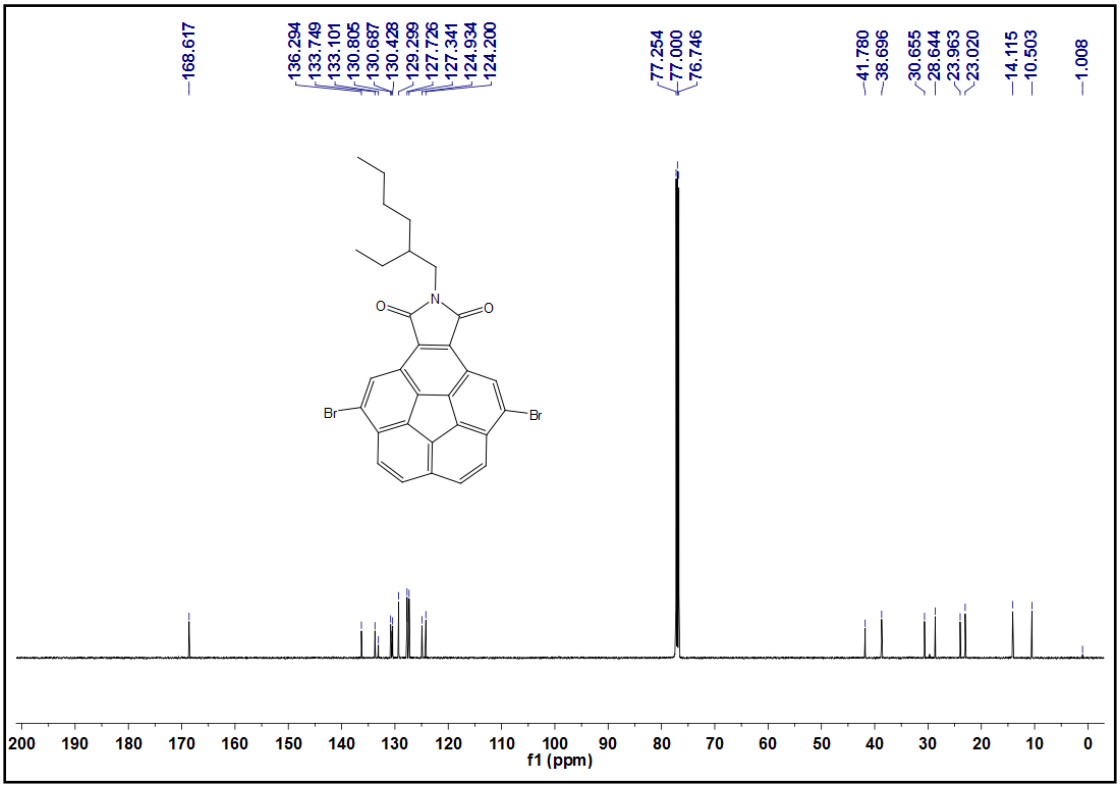
168.617
136.294
133.749
133.101
130.805
130.687
130.428
129.299
127.726
127.341
124.934
124.200
77.254
77.000
76.746
41.780
38.696
30.655
28.644
23.963
23.020
14.115
10.503
1.008
f1 (ppm)

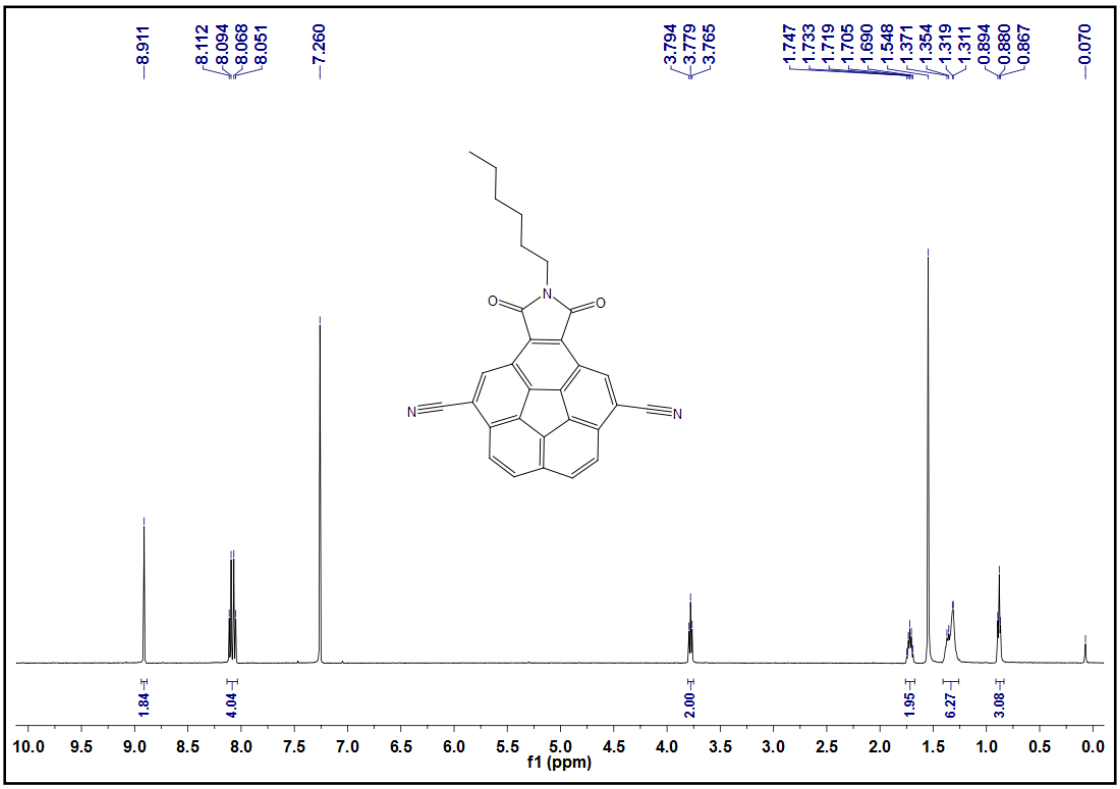
8.911
8.112
8.094
8.068
8.051
7.260
3.794
3.779
3.765
1.747
1.733
1.719
1.705
1.690
1.548
1.371
1.354
1.319
1.311
0.894
0.880
0.867
0.070
1.84
4.04
2.00
1.95
6.27
3.08
f1 (ppm)

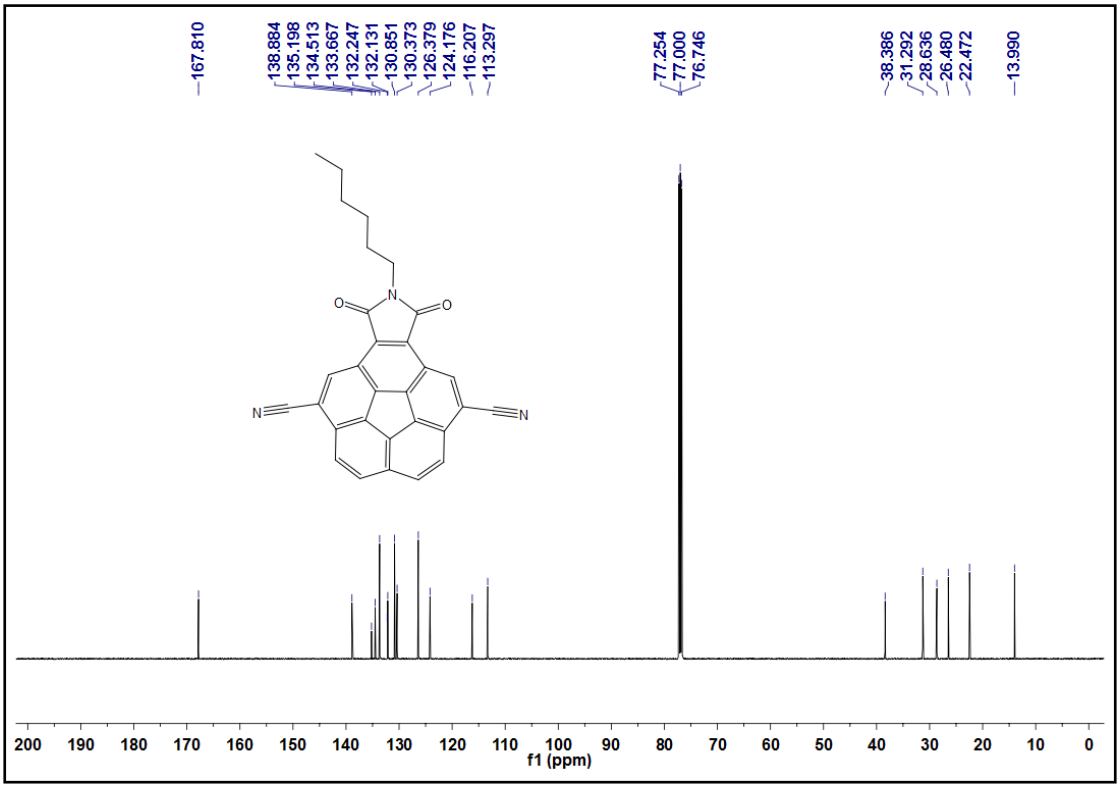
167.810
138.884
135.198
134.513
133.667
132.247
132.131
130.851
130.373
126.379
124.176
116.207
113.297
77.254
77.000
76.746
38.386
31.292
28.636
26.480
22.472
13.990
f1 (ppm)

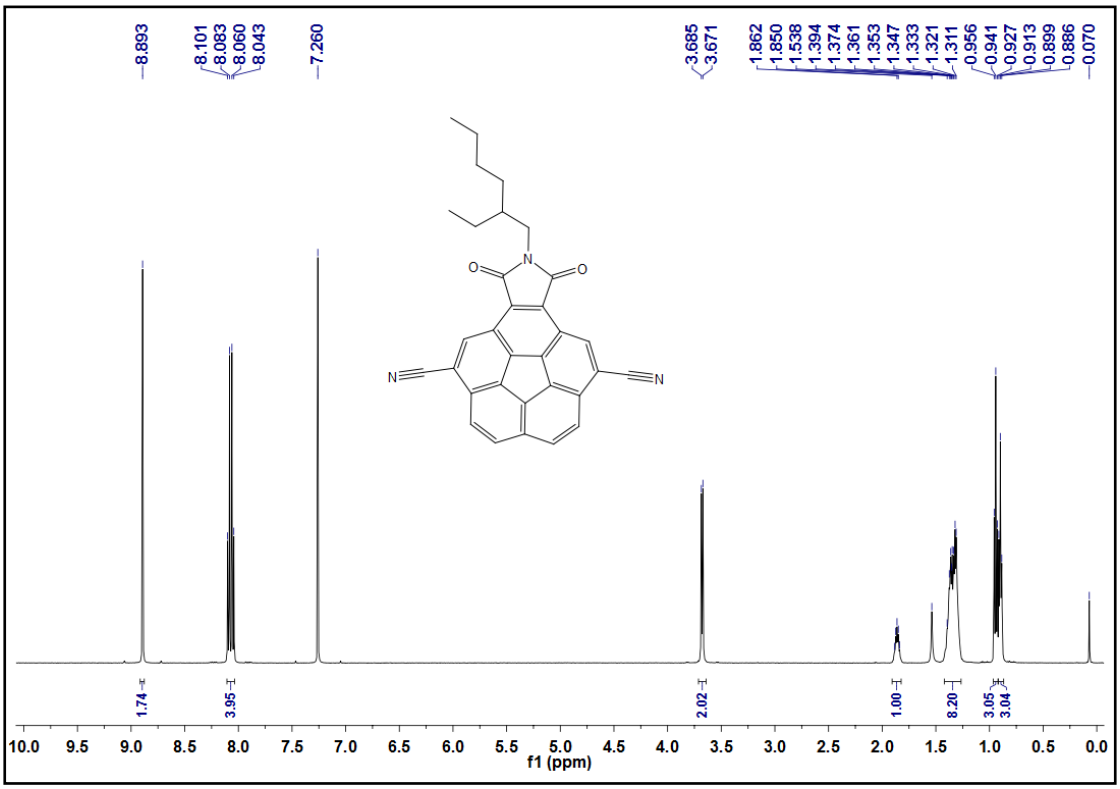

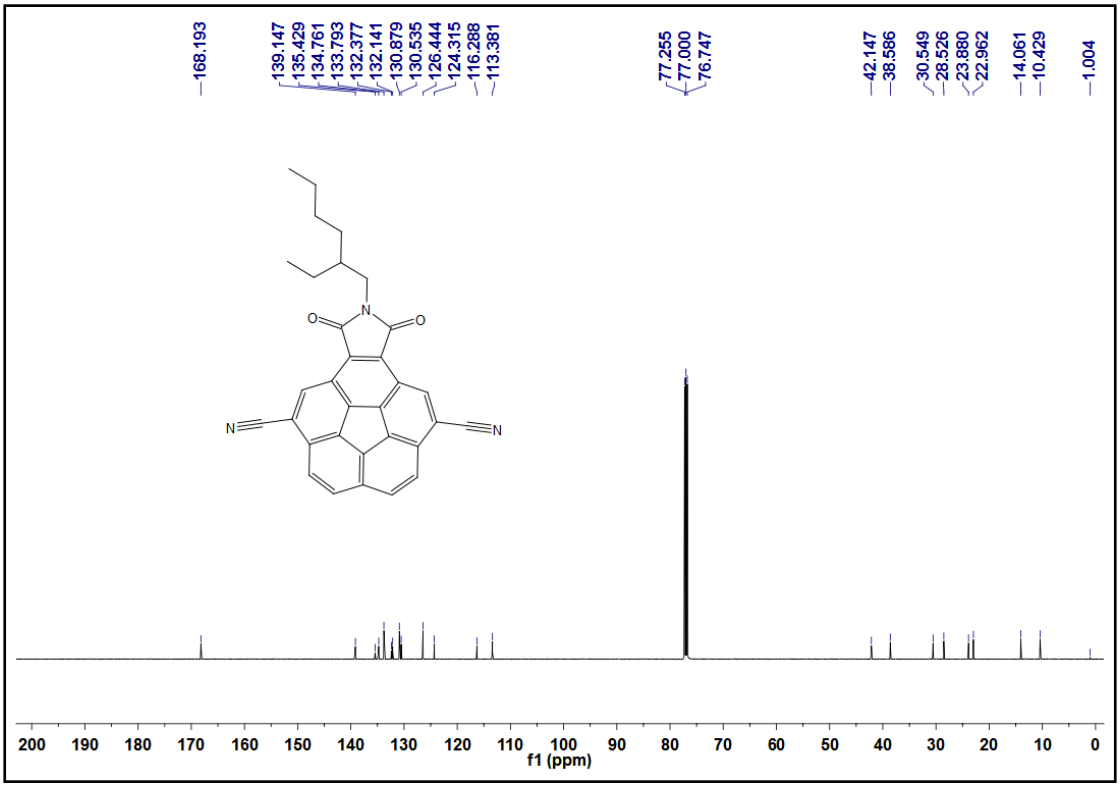

11. Reference

1 S. Demmig and H. Langhals, *Chem. Ber.*, 1988, **121**, 225.

2 M. J. Tauber, R. F. Kelley, J. M. Giaimo, B. Rybtchinski and M. R. Wasielewski, *J. Am. Chem. Soc.*,
2006, **128**, 1782.

3 B. A. Jones, A. Facchetti, M. R. Wasielewski and T. J. Marks, *J. Am. Chem. Soc.*, 2007, **129**, 15259.

4 Gaussian 09, Revision B.01, M. J. Frisch, G. W. Trucks, H. B. Schlegel, G. E. Scuseria, M. A. Robb, J. R. Cheeseman, G. Scalmani, V. Barone, B. Mennucci, G. A. Petersson, H. Nakatsuji, M. Caricato, X. Li, H. P. Hratchian, A. F. Izmaylov, J. Bloino, G. Zheng, J. L. Sonnenberg, M. Hada, M. Ehara, K. Toyota, R. Fukuda, J. Hasegawa, M. Ishida, T. Nakajima, Y. Honda, O. Kitao, H. Nakai, T. Vreven, J. A. Montgomery, Jr., J. E. Peralta, F. Ogliaro, M. Bearpark, J. J. Heyd, E. Brothers, K. N. Kudin, V. N. Staroverov, R. Kobayashi, J. Normand, K. Raghavachari, A. Rendell, J. C. Burant, S. S. Iyengar, J. Tomasi, M. Cossi, N. Rega, J. M. Millam, M. Klene, J. E. Knox, J. B. Cross, V. Bakken, C. Adamo, J. Jaramillo, R. Gomperts, R. E. Stratmann, O. Yazyev, A. J. Austin, R. Cammi, C. Pomelli, J. W. Ochterski, R. L. Martin, K. Morokuma, V. G. Zakrzewski, G. A. Voth, P. Salvador, J. J. Dannenberg, S. Dapprich, A. D. Daniels, Ö. Farkas, J. B. Foresman, J. V. Ortiz, J. Cioslowski, and D. J. Fox, Gaussian, Inc., Wallingford CT, 2009.

5 C. F. Guerra, J. Snijders, G. Te Velde and E. Baerends, *Theor. Chem. Acc.* 1998, **99**, 391.

6 G. Te Velde, F. M. Bickelhaupt, E. J. Baerends, C. Fonseca Guerra, S. J. van Gisbergen, J. G. Snijders and Ziegler, T. *Comp. Chem.* 2001, **22**, 931.

7 ADF2014, SCM, Theoretical Chemistry, Vrije Universiteit, Amsterdam, The Netherlands, http://www.scm.com E.J. Baerends, T. Ziegler, J. Autschbach, D. Bashford, A. Bérces, F.M. Bickelhaupt, C. Bo, P.M. Boerrigter, L. Cavallo, D.P. Chong, L. Deng, R.M. Dickson, D.E. Ellis, M. van Faassen, L. Fan, T.H. Fischer, C. Fonseca Guerra, M. Franchini, A. Ghysels, A. Giammona, S.J.A. van Gisbergen, A.W. Götz, J.A. Groeneveld, O.V. Gritsenko, M. Grüning, S. Gusarov, F.E. Harris, P. van den Hoek, C.R. Jacob, H. Jacobsen, L. Jensen, J.W. Kaminski, G. van Kessel, F. Kootstra, A. Kovalenko, M.V. Krykunov, E. van Lenthe, D.A. McCormack, A. Michalak, M. Mitoraj, S.M. Morton, J. Neugebauer, V.P. Nicu, L. Noodleman, V.P. Osinga, S. Patchkovskii, M. Pavanello, P.H.T. Philipsen, D. Post, C.C. Pye, W. Ravenek, J.I. Rodríguez, P. Ros, P.R.T. Schipper, H. van Schoot, G. Schreckenbach, J.S. Seldenthuis, M. Seth, J.G. Snijders, M. Solà, M. Swart, D. Swerhone, G. te Velde, P. Vernooijs, L. Versluis, L. Visscher, O. Visser, F. Wang, T.A. Wesolowski, E.M. van Wezenbeek, G. Wiesenekker, S.K. Wolff, T.K. Woo, A.L. Yakovlev.

8 B. M. Schmidt, B. Topolinski, P. Roesch and D. Lentz, *Chem. Commun.*, 2012, **48**, 6520.